Available online at www.sciencedirect.com
SCIENCE DIRECT®
Electrochimica Acta 50 (2005) 2249–2254
ELECTROCHIMICA Acta
www.elsevier.com/locate/electacta

Nafion®-assisted deposition of microemulsion-synthesized platinum nanoparticles on BDD Activation by electrogenerated •OH radicals

G. Siné, Ch. Comninellis*,[1]

SB-ISIC-GGEC, Ecole Polytechnique Fédérale de Lausanne (EPFL), CH-1015 Lausanne, Switzerland

Received 15 June 2004; received in revised form 15 September 2004; accepted 2 October 2004
Available online 11 November 2004

Abstract

Platinum nanoparticles have been synthesized by the water-in-oil (w/o) microemulsion technique and deposited onto boron-doped diamond (BDD) electrodes. Transmission electron microscopy (TEM) has shown that Pt particles size is limited to 2–5 nm range with narrow distribution. Anodic treatment at high overpotentials activates Pt deposit that is mechanically stabilized by a Nafion® layer. Such activation results in enhancement of activity towards methanol electrooxidation, due to additional cleaning of the particles by oxidation of the residual surfactant by electrogenerated hydroxyl radicals.

Keywords: Microemulsion; Pt nanoparticles; Nafion® film; Hydroxyl radicals electrogenerated on diamond electrode; Methanol electrooxidation

1. Introduction

Since a few decades, there is a growing interest in the study of supported catalyst nanoparticles (Pt, Ru, IrO_2, RuO_2) due to the different and, sometimes, novel properties of the later compared to bulk materials. Special attention was focused on Pt nanoparticles due to their applicability for the Direct Alcohol Fuel Cell (DAFC) technology [1,2]. However, the complete oxidation of methanol to carbon dioxide passes through several adsorbed intermediates [3] and CO poisoning that blocks methanol adsorption onto reactive sites dramatically decreases the activity of the catalyst [4]. Alloying Pt with other transition metals (Ru, Sn, Mo, W or Ni) enhances CO tolerance of pure Pt, but the reasons are still under debate. Two approaches are currently privileged by researchers: the so-called bifunctional mechanism [5], during which Pt adsorbs methanol, and the other metal dissociates water molecules at lower overpotentials than Pt, and the electronic effect, in which the Pt–CO bond is weakened by the modification of electronic properties of Pt induced by the presence of the alloying metal [6]. On the other hand, the necessity of alloying metals instead of just mixing them is now an open question [7]. Special requirements in catalysis science consist in obtaining monodispersed nanoparticles with well-defined compositions. The microemulsion method is well known, since the first work of Boutonnet et al. [8], to be an efficient and simple way to prepare metallic particles in the nanometer scale with narrow size distribution. A water-in-oil (w/o) microemulsion is a thermodynamically stable, optically transparent and isotropic dispersion of aqueous nanodroplets coated by a layer of surfactant in a continuous oily phase [9]. This method has been successfully used for the synthesis of nanomaterials like pure metals [8,10], alloys [11–13] or metal oxides [14]. However, the surfactant layer that limits the particles growth to the droplets own dimensions becomes a problem for their electrochemical and electrocatalytic characterization. Thus cleaning of such synthesized

* Corresponding author. Tel.: +41 21 693 36 74; fax: +41 21 693 31 90.
E-mail addresses: guillaume.sine@epfl.ch (G. Siné), christos.comninellis@epfl.ch (Ch. Comninellis).
[1] ISE member.

0013-4686/$ – see front matter © 2004 Elsevier Ltd. All rights reserved.
doi:10.1016/j.electacta.2004.10.008

particles appears as a major challenge in order to allow their electrochemical study. Electrochemical aging or activation (i.e. potential sweep between typically 0 and 1.3–1.5 V versus SHE) has been used to clean Pt surfaces but it implies surface rearrangements or recombination [15], and aggregation of particles [16]. Recently, a cleaning procedure that includes CO adsorption and stripping has been successfully used for the decontamination of Pt-based nanoparticles prepared in microemulsion systems [17,18].

We have recently started some investigations on BDD-supported Pt and Pt-based nanoparticles synthesized via the microemulsion technique. The main advantages of BDD as support consist in the inert character of its surface, a very low background current and a large electrochemical window available [19], and the BDD electrode has been widely studied for its use on electrochemical oxidation of organic pollutants [20–22]. The use of BDD as substrate can be a good approach to solve the problems of corrosion (glassy carbon) or oxide formation (Au and Ti) encountered with usual substrates, problems that can result in the modification of the catalytic activity of the deposited particles (metal–support interactions). Diamond substrates have thus been used as substrate for the deposition of various metallic particles including mercury and silver [23], lead dioxide [24], ruthenium oxides [25,26] or gold [27]. In most of the papers dealing with BDD-supported platinum particles, electrodeposition was the employed technique, but yields to particles with a large size distribution and that cannot be considered strictly as nanoparticles (i.e. $d > 100$ nm) [28,29].

In the present article, we report some preliminary results obtained for pure platinum nanoparticles, which can be activated by electrogenerated hydroxyl radicals on BDD. It was indeed showed in a recent paper from our laboratory [30] that free and highly reactive hydroxyl radicals are produced on BDD electrodes by water discharge at high overpotentials (>2.3 V versus SHE), as described in Eq. (1):

$$H_2O \rightarrow {}^{\bullet}OH + H^+ + e^- \quad (1)$$

These electrogenerated hydroxyl radicals at the BDD surface participate in the oxidation of the residual surfactant layer present on the Pt nanoparticles, resulting in a clean surface. Furthermore, in order to avoid detachment of Pt nanoparticles during this treatment, we have also considered the use of a Nafion® film to mechanically stabilize these ones, following a similar way than Swain et al. who entrapped their particles in an additional diamond layer [31,32].

2. Experimental

2.1. Nanoparticles synthesis

Platinum nanoparticles were obtained by reduction of H_2PtCl_6 with hydrazine in a w/o microemulsion of water/tetraethyleneglycol-monododecylether (BRIJ® 30)/*n*-heptane, following Eq. (2):

$$H_2PtCl_6 + NH_2NH_2 \rightarrow Pt + 6HCl + N_2 \quad (2)$$

The microemulsions were prepared using ultra-pure water (Millipore® system). BRIJ® 30 and *n*-heptane were purchased from Fluka and Riedel-de-Haën, respectively, and were used as received. The reactants (Fluka, analytical grade) were dissolved into the aqueous phases of two different microemulsions that had the same composition and water-to-surfactant ($\omega_0 = 3.8$) molar ratio. The quantity of surfactant represented 16.54% of the volume of the microemulsion, and the concentrations of H_2PtCl_6 and hydrazine in the aqueous phases were 0.1 and 2.5 M, respectively. The synthesis was realised mixing equal volumes of the two microemulsions. After complete reduction, acetone was added to the solution to cause phase separation and precipitation of the particles. The precipitate was rinsed several times with acetone and ultra-pure water, and then centrifuged for a few minutes to eliminate most of the surfactant. Finally, particles were put in a small volume of ultra-pure water as a suspension.

2.2. Electrode preparation

BDD films were synthesized by the hot filament chemical vapor deposition technique (HF-CVD) on single crystal p-type Si ⟨1 0 0⟩ wafers (1–3 mΩ cm, Siltronix). The doping level of boron expressed as B/C ratio was about 3500 ppm. The obtained diamond film thickness was about 1 μm with a resistivity in the range 10–30 mΩ cm. This as-grown BDD contains some graphitic (sp^2) phase and is hydrogen terminated. Activation of BDD by anodic polarization (10 mA cm^{-2} in 1 M H_2SO_4 at 25 °C during 30 min) eliminates most of the sp^2 and adsorbed hydrogen from the surface, and is necessary to obtain reproducible electrochemical measurements [33].

Platinum nanoparticles were deposited onto the BDD substrate putting a droplet (5 μl) of the suspension onto diamond. The excess water was dried under nitrogen atmosphere. The BDD–Pt–Nafion® electrode was realized adding 5 μl of a commercial solution of Nafion® (5 wt.% in aliphatic alcohols, Aldrich), diluted ten more times in pure ethanol, to the BDD–Pt electrode. The excess alcohol was also removed under nitrogen atmosphere. The BDD–Pt or BDD–Pt–Nafion® electrode was then transferred to the electrochemical cell.

2.3. Measurements

Electrochemical measurements were performed in a conventional three-electrode cell using a computer-controlled EG&G potentiostat model M 273. BDD–Pt or BDD–Pt–Nafion® (exposed area of BDD: 0.4 cm^2) was used as working electrode, $Hg/Hg_2SO_4{\cdot}K_2SO_4$ (saturated) as reference and Pt wire as counter electrode. All potentials in this work are referred with respect to the Standard Hydrogen Electrode (SHE). All solutions were made with ultra-pure

water and analytical grade reagents, and were saturated with nitrogen gas prior to each experiment.

Transmission Electron Microscopy (TEM) analyses were conducted using a Philips CM 300 microscope. A small droplet of the aqueous particles suspension was deposited onto an amorphous carbon-coated copper grid, and the excess water was removed before analysis. Atomic absorption spectroscopy (AAS) was also used to determine the concentration of Pt particles in the suspension.

3. Results and discussion

The principle of nanoparticle synthesis by the microemulsion method is schematised in Fig. 1. The synthesis involves the following steps: (1) mixing of two w/o microemulsions of identical formulation, each one containing one of the reactant (H_2PtCl_6 and N_2H_4) dissolved in its aqueous phase, (2) collision between aqueous droplets due to Brownian motion, formation of metastable fused dimers and exchange of reactants, (3) nucleation of Pt clusters after reduction of Pt^{2+} ions with hydrazine (see Eq. (2)), and (4) growth of the particles into the inverse micelles.

A TEM micrograph of Pt particles synthesized in w/o microemulsion system is shown in Fig. 2. It can be seen from this picture that Pt particles are present on the copper grid as small spherical isolated units. The size domain of these units is limited to the range 2–5 nm that corresponds well with the commonly accepted definition of a nanoparticle in electrocatalysis.

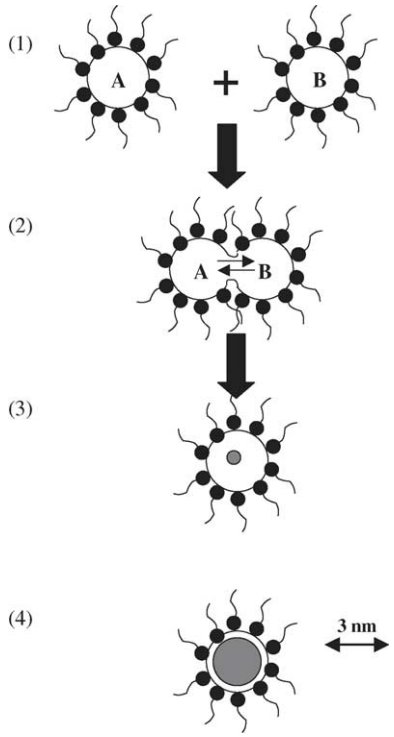

Fig. 1. Schematic representation of nanoparticles synthesis by the w/o microemulsion technique: (1) mixing of the two microemulsions; (2) collision between droplets, exchange of reactants and reduction of H_2PtCl_6 following Eq. (2); (3) nucleation of Pt and (4) growth of the Pt particles into the aqueous droplets. A: H_2PtCl_6 aq., B: N_2H_4 aq.; inverse micelles containing the reactants are dispersed into an *n*-heptane phase and stabilized by a surfactant (BRIJ® 30 of molecular formula $C_{12}H_{25}(OCH_2CH_2)_4OH$) layer.

The cleaning of BDD–Pt and BDD–Pt–Nafion® electrodes under potential conditions for which hydroxyl radicals are produced on BDD has been investigated. For this purpose, a potential of 2.5 V versus SHE was applied in 1 M $HClO_4$ to the BDD–Pt electrode during a determined time. The potential was then cycled until a stable voltammogram was obtained and the charge in the H adsorption–desorption region was calculated. Fig. 3 shows the evolution of the normalized charge versus time of activation treatment for a BDD–Pt (thin line with triangle markers) and a BDD–Pt–Nafion® (thick line with square markers) electrode. The decreases with time of treatment indicate detachment of particles from the substrate caused by oxygen evolution on BDD. Nevertheless, this phenomenon is less pronounced when the polymer layer is added and the beneficial effect of Nafion® on the stability of the Pt deposit on BDD is clearly visible. A zoom onto the 0–5 s domain is given in *inset* of Fig. 3. The initial increase of charge for the BDD–Pt–Nafion® electrode can be related to cleaning of the surface, i.e. oxidation of the residues of surfactant by electrogenerated hydroxyl radicals at the BDD electrode, whereas non-coated Pt is immediately removed in important quantities. It seems possible in the case of the BDD–Pt–Nafion® electrode to define an optimum activation time of approximately 3 s. The CV of the BDD–Pt–Nafion® electrode recorded in $HClO_4$ 1 M after 0 s (thin line) and 3 s (thick line) of activation at 2.5 V are shown in Fig. 4. After activation, the Pt signal exhibits better-defined H adsorption–desorption peaks of higher intensities, indicating that the process effectively cleans the surface.

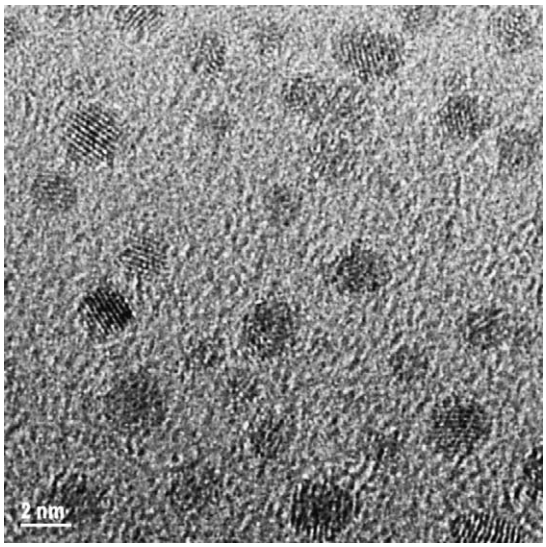

Fig. 2. TEM micrograph of platinum nanoparticles synthesized by the microemulsion method.

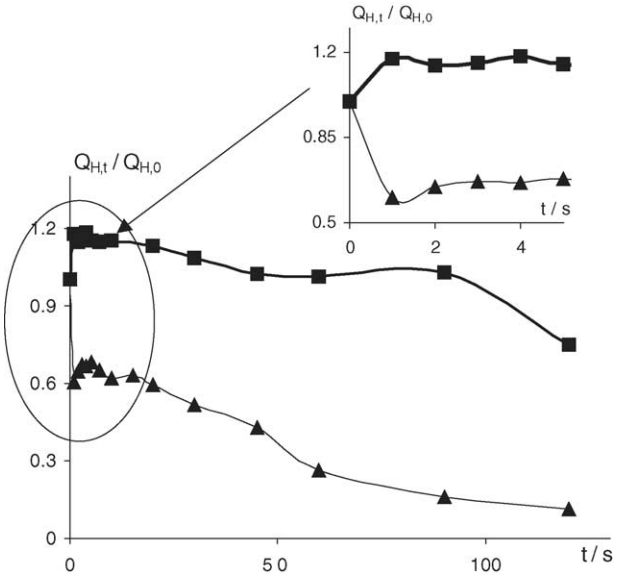

Fig. 3. Evolution of normalized charge in the H adsorption–desorption region of Pt on a BDD–Pt (thin line with triangle markers) and a BDD–Pt–Nafion (thick line with square markers) electrode vs. time of activation at 2.5 V vs. SHE. Scan rate of 50 mV s^{-1} in 1 M $HClO_4$ at 25 °C. *Inset*: zoom on the 0–5 s domain.

The catalytic activity of the BDD–Pt electrode was tested both for methanol and ethanol electrooxidations that are the main reactions of interest for the DAFC technology. CV of a BDD–Pt (thin lines) and of a BDD–Pt–Nafion® (thick lines) electrode in $HClO_4$ 1 M + CH_3OH 0.1 M and $HClO_4$ 1 M + C_2H_5OH 0.1 M solutions, recorded at a scan rate of 50 mV s^{-1}, are shown in Fig. 5a and b, respectively. The voltammograms of Fig. 5 exhibit the characteristic features of methanol and ethanol oxidations on pure platinum. The CV of methanol electrooxidation can for instance be described as a sequence of multiple and complex physicochemical phenomena [34]. At very low overpotentials (0.05 V versus SHE), methanol easily adsorbs on Pt, adsorption that is followed by alcohol dehydrogenation (during a fast process) as described

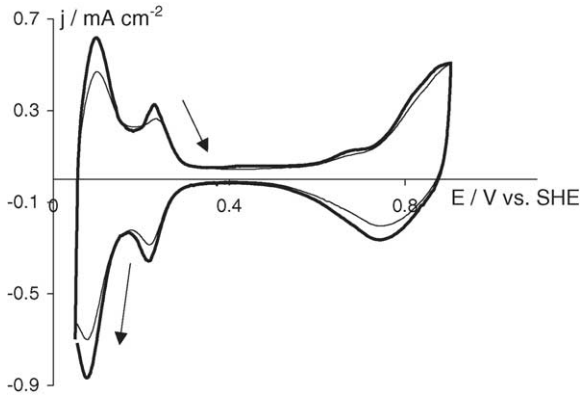

Fig. 4. Cyclic voltammograms of a BDD–Pt–Nafion® electrode after 0 s (thin line) and 3 s (thick line) of activation at 2.5 V vs. SHE. Scan rate of 50 mV s^{-1} in 1 M $HClO_4$ at 25 °C.

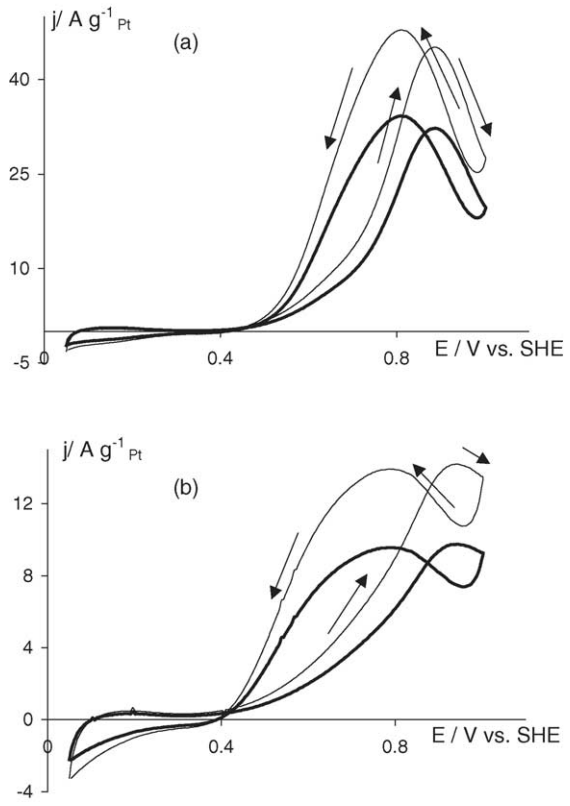

Fig. 5. Cyclic voltammograms of a BDD–Pt (thin lines) and a BDD–Pt–Nafion® (thick lines) electrode in the presence of methanol (a) and ethanol (b). Scan rate of 50 mV s^{-1} in 1 M $HClO_4$ + 0.1 M CH_3OH at 25 °C (a), and in 1 M $HClO_4$ + 0.1 M C_2H_5OH at 25 °C (b).

in reactions (3.1) and (3.2):

$$3Pt(H_2O) + CH_3OH \rightarrow Pt_3(CH_3OH)_{ads} + 3H_2O \quad (3.1)$$

$$Pt_3(CH_3OH)_{ads} \rightarrow Pt(CO)_{ads} + 2Pt + 4H^+ + 4e^- \quad (3.2)$$

As a consequence, carbon monoxide (CO) blocks the Pt active sites, explaining the flat feature of CV of Fig. 5a between 0.05 and 0.45 V versus SHE, approximately. CO to be removed needs to be oxidized by hydroxyl radicals generated from water discharge on Pt. However, water dissociation does not occur on Pt at potentials below 0.4 V versus SHE. When this potential is attained, the following sequence can take place (reactions (4.1) and (4.2)):

$$Pt + H_2O \rightarrow Pt(^{\bullet}OH)_{ads} + H^+ + e^- \quad (4.1)$$

$$Pt(CO)_{ads} + Pt(^{\bullet}OH)_{ads} \rightarrow 2Pt + CO_2 + H^+ + e^- \quad (4.2)$$

This explains the current increase after 0.45 V: Pt can readsorb and reoxydate methanol. The current decrease after 0.9 V versus SHE can be related to the Pt surface state: cycling the potential in acidic media up to 1 V versus SHE and more, Pt oxides formation begins. Consequently, there is no Pt free to dissociate water and the current decreases. During the reverse scan of potential, Pt oxides are reduced, so water

dissociation and methanol complete oxidation can take place again. Finally, the current decreases again due to CO poisoning of the surface when the potential is not sufficiently high to allow water dissociation. The second oxidation peak is of higher intensity than the first one and located at less positive potential because this second oxidation takes place on a "fresh" Pt surface that is more active.

A similar mechanism should be theoretically expected in the case of ethanol electrooxidation, however, ethanol complete electrooxidation is a much more complicated case as it needs the breaking of the C–C bond. On platinum, this reaction first yields to several adsorbed intermediates, namely acetaldehyde and acetic acid that have been identified by means of Fourier transform infra-red spectroscopy (FTIR) [35,36]. The breaking of the C–C bond of these adsorbates is one of the key problems in ethanol-feed DAFC. A good electrocatalyst for the complete oxidation of ethanol is indeed defined as an activator of the C–C bond breaking [37]. Thus, we can reasonably postulate that difference in activity of Pt particles towards the oxidation of methanol and ethanol is due to the inability of pure Pt to promote the breaking of the C–C bond of ethanol. This incomplete oxidation would lead to acetaldehyde and/or acetic acid that only need two electrons per molecule of adsorbate formed. This explains the fact that in Fig. 5, activity of Pt is three times more important towards methanol electrooxidation, and that the oxidation current peaks are located at approximately 0.9 (forward scan) and 0.75 V versus SHE (reverse scan) for methanol oxidation, and at 0.95 (forward) and 0.8 V versus SHE (reverse) for ethanol oxidation.

It can also be seen in Fig. 5 that the intensities of CV for the coated electrode corresponds to 70% of the signal of the non-coated one, due to partial blockage of the catalytic surface by the polymer. Nevertheless, Nafion® does not affect peaks shapes and positions. The same observations were made from CV measured in pure supporting electrolyte (data not shown).

Fig. 6 shows the evolution of normalized oxidation current peaks for methanol electrooxidation with and without the Nafion® adlayer. For clarity, only the evolution of the first oxidation peak (during the forward potential scan) is shown here, but the same tendency is also observed, with lower levels of increase, for the second one. Without Nafion®, the curve of methanol oxidation (thin line with triangle markers in Fig. 6) begins with a strong increase followed by a continuous decrease. When the polymer is added (thick line with square markers in Fig. 6), the initial increase of activity is of higher importance and the decrease with time is limited. Initial enhancement of catalytic activity can be due to assistance of oxidation by hydroxyl radicals when the polymer is absent, and by combination of this process with additional cleaning of the particles when Nafion® is present. The final decrease in activity can be related to the loss of catalytic material. Zooming on the 0–5 s region allows the definition of an optimum activation time of 4 s.

CV of a BDD–Pt–Nafion® recorded in 1 M $HClO_4$ + 0.1 M CH_3OH at 20 mV s^{-1} before (thin line) and after activation

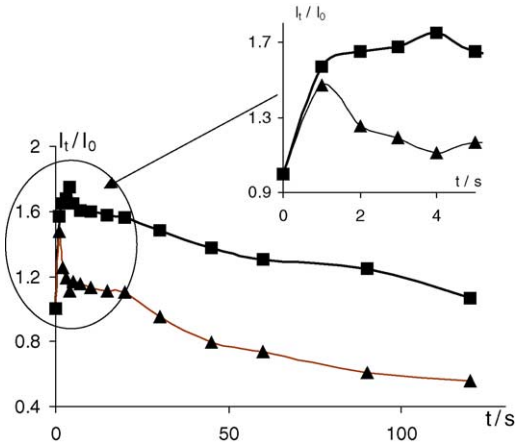

Fig. 6. Evolution of normalized first oxidation peak currents of methanol on a BDD–Pt (thin lines with triangle markers) and a BDD–Pt–Nafion® (thick lines with square markers) electrode vs. time of activation at 2.5 V vs. SHE. Scan rate of 20 mV s^{-1} in 1 M $HClO_4$ + 0.1 M CH_3OH at 25 °C. *Inset*: zoom on the 0–5 s domain.

(4 s at 2.5 V versus SHE) are shown in Fig. 7. It can be seen that the onset of first oxidation peak is shifted to less positive potentials by the activation procedure whereas the second oxidation peak position is not changed. It can also be noticed that after activation, the first oxidation peak intensity is much important that the second one. Such behaviour can be explained by the fact that electrogenerated •OH radicals on BDD may spillover onto the Pt surface, participating in the methanol oxidation process itself and explaining both the increase in oxidation current and the shift in peak position. The oxidation peak recorded during the reverse scan is of lower intensity than the first one, certainly due to the fact that all the electrogenerated free hydroxyl radicals were consumed during the forward scan. The current measured during the reverse scan is only due to the Pt deposit and assistance of the oxidation process by •OH radicals may not occur. Nevertheless, the catalyst surface is more active than it was before activation. Similar behaviour is also observed in the case of ethanol electrooxidation (data not shown).

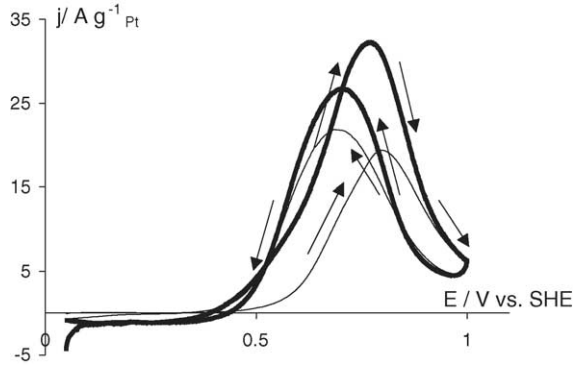

Fig. 7. Cyclic voltammograms of a BDD–Pt–Nafion® electrode after 0 s (thin line) and 4 s (thick line) of activation at 2.5 V vs. SHE. Scan rate of 20 mV s^{-1} in 1 M $HClO_4$ + 0.1 M CH_3OH at 25 °C.

4. Conclusion

The microemulsion method is a simple, efficient way to produce platinum or metallic nanoparticles. TEM analyses have revealed that the size of such synthesized Pt particles is included in the 2–5 nm range that corresponds well with the definition of a nano-object in catalysis. Activation of the Pt deposit by hydroxyl radicals produced by water discharge becomes feasible when a Nafion® layer is added to the BDD–Pt electrode. The polymer layer strongly stabilizes the particles under these conditions, and optimum activation times, for which activity reaches by a maximum, have been found to be close to 3 s in all cases. Enhancement of activity thanks to activation by hydroxyl radicals can be attributed to the combination of two effects: cleaning of particles from the remaining surfactant and assistance of the electrooxidation reaction itself, and is characterized by an increase of oxidation peak currents and a shift of onset of oxidation to lower potentials. With the non-coated electrode, beneficial effect of activation is counterbalanced by important loss of catalytic material.

Further studies will help in investigating the relationship between surface properties of the substrate and behaviour of the Pt deposits, in terms of stability and catalytic activity. We have, for instance, recently reported the possibility to modify BDD characteristics by electrochemical treatment in organic media, leading to polishing and enrichment in C–O bonds of the surface [38]. Current experiments are conducted on platinum-based alloys microemulsion-synthesized nanoparticles. Special attention is focused on Pt/Ru nanoparticles, since they have been designated as the best candidate catalyst for methanol oxidation [39].

Acknowledgements

Authors thank the CSEM Centre Suisse d'Electronique et de Microtechnique SA, Neuchâtel, Switzerland, for preparing the boron-doped diamond electrodes, and Professor Ph. A. Buffat from the Interdisciplinary Centre of Electronic Microscopy (CIME), EPFL, for performing TEM analyses. Financial support from the Fonds National Suisse de la Recherche Scientifique is also gratefully acknowledged.

References

[1] A. Hamnett, in: W. Vielstich, H.A. Gasteiger, A. Lamm (Eds.), Handbook of Fuel Cells—Fundamentals, Technology and Applications, vol. 1, John Wiley & Sons, Ltd., 2003, p. 305.
[2] C. Lamy, E.M. Belgsir, in: W. Vielstich, H.A. Gasteiger, A. Lamm (Eds.), Handbook of Fuel Cells—Fundamentals, Technology and Applications, vol. 1, John Wiley & Sons, Ltd., 2003, p. 323.
[3] T. Iwasita, W. Vielstich, E. Santos, J. Electroanal. Chem. 229 (1987) 367.
[4] P. Waszczuk, A. Wieckowski, P. Zelenay, S. Gottesfeld, C. Coutanceau, J.-M. Leger, C. Lamy, J. Electroanal. Chem. 511 (2001) 55.
[5] M. Watanabe, S. Motoo, J. Electroanal. Chem. 60 (1975) 267.
[6] K.-W. Park, J.-H. Choi, B.-K. Kwon, S.-A. Lee, Y.-E. Sung, H.-Y. Ha, S.-A. Hong, H. Kim, A. Wieckowski, J. Phys. Chem. B 106 (2002) 1869.
[7] L. Dubau, F. Hahn, C. Coutanceau, J.-M. Leger, C. Lamy, J. Electroanal. Chem. 554–555 (2003) 407.
[8] M. Boutonnet, J. Kizling, P. Stenius, Colloids Surf. 5 (1982) 209.
[9] I. Danielsson, B. Lindman, Colloids Surf. 3 (1981) 391.
[10] J. Rymes, G. Ehret, L. Hilaire, M. Boutonnet, K. Jiratova, Catal. Today 75 (2002) 297.
[11] M.-L. Wu, D.-H. Chen, T.-C. Huang, J. Colloid Interface Sci. 243 (2001) 102.
[12] M.-L. Wu, D.-H. Chen, T.-C. Huang, Chem. Mater. 13 (2001) 599.
[13] J. Solla-Gullon, V. Montiel, A. Aldaz, J. Clavilier, Electrochem. Commun. 4 (2002) 716.
[14] K.C. Song, J.H. Kim, Powder Technol. 107 (2000) 268.
[15] J. Clavilier, D. Armand, J. Electroanal. Chem. 199 (1986) 187.
[16] Y. Takasu, Y. Fujii, K. Yasuda, Y. Iwanaga, Y. Matsuda, Electrochim. Acta 34 (1989) 453.
[17] J. Solla-Gullon, V. Montiel, A. Aldaz, J. Clavilier, J. Electroanal. Chem. 491 (2000) 69.
[18] J. Solla-Gullon, V. Montiel, A. Aldaz, J. Clavilier, J. Electrochem. Soc. 150 (2003) E104.
[19] Y.V. Pleskov, in: R.C. Alkire, D.M. Kolb (Eds.), Advances in Electrochemical Science and Engineering, vol. 8, Wiley-VCH, Weinheim, 2002, p. 209.
[20] J. Iniesta, P.-A. Michaud, M. Panizza, G. Cerisola, A. Aldaz, Ch. Comninellis, Electrochim. Acta 46 (2001) 3573.
[21] M. Panizza, P.A. Michaud, G. Cerisola, Ch. Comninellis, J. Electroanal. Chem. 507 (2001) 206.
[22] M.A. Rodrigo, P.-A. Michaud, I. Duo, M. Panizza, G. Cerisola, Ch. Comninellis, J. Electrochem. Soc. 148 (2001) D60.
[23] N. Vinokur, B. Miller, Y. Avyigal, R. Kalish, J. Electrochem. Soc. 146 (1999) 125.
[24] A.J. Saterlay, S.J. Wilkins, K.B. Holt, J.S. Foord, R.G. Compton, F. Marken, J. Electrochem. Soc. 148 (2001) E66.
[25] S. Ferro, A. De Battisti, J. Phys. Chem. B 106 (2002) 2249.
[26] K.J. McKenzie, F. Marken, Electrochem. Solid-State Lett. 5 (2002) E47.
[27] Y. Zhang, S. Asahina, S. Yoshibira, T. Shirakashi, Electrochim. Acta 48 (2003) 741.
[28] O. Enea, B. Riedo, G. Dietler, Nano Lett. 2 (2002) 241.
[29] F. Montilla, E. Morallon, I. Duo, Ch. Comninellis, J.L. Vazquez, Electrochim. Acta 48 (2003) 3891.
[30] B. Marselli, J. Garcia-Gomez, P.-A. Michaud, M.A. Rodrigo, Ch. Comninellis, J. Electrochem. Soc. 150 (2003) D79.
[31] J. Wang, G.M. Swain, T. Tachinaba, K. Kobashi, Electrochem. Solid-State Lett. 3 (2000) 286.
[32] J. Wang, G.M. Swain, J. Electrochem. Soc. 150 (2003) E24.
[33] D. Gandini, E. Mahé, P.-A. Michaud, W. Haenni, A. Perret, Ch. Comninellis, J. Appl. Electrochem. 30 (2000) 1345.
[34] M.P. Hogarth, T.R. Ralph, Platinum Met. Rev. 46 (2002) 146.
[35] B. Beden, M.-C. Morin, F. Hahn, C. Lamy, J. Electroanal. Chem. 229 (1987) 353.
[36] J.M. Perez, B. Beden, F. Hahn, A. Aldaz, C. Lamy, J. Electroanal. Chem. 262 (1989) 251.
[37] F. Vigier, C. Coutanceau, F. Hahn, E.M. Belgsir, C. Lamy, J. Electroanal. Chem. 563 (2004) 81.
[38] M. Panizza, G. Siné, I. Duo, L. Ouattara, Ch. Comninellis, Electrochem. Solid-State Lett. 6 (2003) D17.
[39] H.A. Gasteiger, N. Markovic, P.N. Ross, E.J. Cairns, Electrochim. Acta 39 (1994) 1825.